

Electron Electric Dipole Moment from Lepton Flavor Violation

Seyed Yaser Ayazi and Yasaman Farzan

Institute for studies in Theoretical Physics and Mathematics (IPM)

P.O. Box 19395-5531, Tehran, Iran

Abstract

The general Minimal Supersymmetric Standard Model introduces new sources for Lepton Flavor Violation (LFV) as well as CP-violation. In this paper, we show that when both sources are present, the electric dipole moment of the electron, d_e , receives a contribution from the phase of the trilinear A -term of staus, $\phi_{A\tau}$. For $\phi_{A\tau} = \pi/2$, the value of d_e , depending on the ratios of the LFV mass elements, can range between zero and three orders of magnitude above the present bound. We show that the present bound on d_e rules out a large portion of the CP-violating and the LFV parameter space which is consistent with the bounds on the LFV rare decays. We show that studying the correlation between d_e and the P-odd asymmetry in $\tau \rightarrow e\gamma$ helps us to derive a more conclusive bound on $\phi_{A\tau}$. We also discuss the possibility of cancelation among the contributions of different CP-violating phases to d_e .

1 Introduction

As is well-known, elementary particles can possess electric dipole moments only if CP is violated. In the framework of the Standard Model (SM) of the elementary particles, the 3×3 quark mixing matrix (the CKM matrix) can accommodate a CP-violating phase. In fact, CP-symmetry in the meson system has been observed to be violated in accord with the SM. However,

the effect of the CP-violating phase of the CKM matrix on the Electric Dipole Moment (EDM) of the electron, d_e , is shown to be very small [1] and beyond the reach of experiments in the foreseeable future [2, 3]. Thus if the forthcoming [3] or proposed experiments detect a nonzero d_e , it will be an indication of physics beyond the SM.

Recent neutrino data proves that Lepton Flavor (LF) has been violated in nature. The effect can be explained by mixing in the neutrino mass matrix. In principle such a LF Violation (LFV) in neutrino mass matrix can lead to the LFV decays, $\tau \rightarrow e\gamma$, $\tau \rightarrow \mu\gamma$ and $\mu \rightarrow e\gamma$ [4]. However, if the neutrino mass matrix is the only source of LFV, the branching ratio of these decays will be so small that cannot be detected in foreseeable future. In the future, if experiments report a nonzero branching ratio for any of the aforementioned LFV decays [5], we will conclude that the SM has to be augmented to include more sources of LFV. In the context of Minimal Supersymmetric Standard Model (MSSM), which is arguably the most popular extension of the SM, there are several sources for CP-violation as well as for LFV which can lead to effects exceeding the present experimental bounds. The bounds on $\text{Br}(\ell_j \rightarrow \ell_i\gamma)$ constrain the sources of LFV in the MSSM. Moreover, the bounds on the EDM of the elementary particles constrain the CP-violating phases of the MSSM. For vanishing LFV sources, the bounds from the EDMs on the CP-violating phases of MSSM parameters have been extensively studied in the literature (for an incomplete list see) [6, 7, 8]. In [9], the effects of the phases of LFV masses as well as the LFV trilinear A -couplings on d_e have been studied. However, [9] does not discuss the possible effects of the phase of A_τ (the trilinear supersymmetry breaking coupling of stau). Notice that although A_τ is a LF conserving coupling which deals only with the staus, in the presence of LFV, it can affect the properties of leptons of other generations.

In this paper, taking into account the possibility of the LFV in soft super-

symmetry breaking terms, we will focus on the possible effects of the phase of A_τ on the electric dipole moment of the electron. As is well-known, the phase of A_τ , ϕ_{A_τ} , can also manifest itself in the decay and production of staus [10]. One of the goals of the proposed state-of-the-art ILC project is detecting such effects [11]. It is therefore very exciting to learn about the value of ϕ_{A_τ} by present or forthcoming low energy experiments.

We show that for $\text{Br}(\tau \rightarrow e\gamma)$ close to its present bound, the bound on d_e can already constrain ϕ_{A_τ} . We discuss how other sets of the CP-violating phases can mimic the effect of ϕ_{A_τ} on d_e and suggest some ways to resolve the degeneracies. Recently, it has been shown in [12] that by measuring the spin of the final particles in the LFV rare decays, one can extract information on the CP-violating phases of the underlying theory. In the present paper, we however do not take into account such a possibility and focus on the spin-averaged decays rate.

The paper is organized as follows. In Sec. 2, we specify the model that we study in this paper and summarize the observable effects that can be used to extract information on the parameters of the model. In Sec. 3, we discuss how CP-violating and LFV parameters affect d_e and other observable quantities and present scatter plots that explore the parameter space. In Sec. 4, we first enumerate the possible CP-violating phases and evaluate their respective effects with special emphasis on the possibility of cancelation. Section 5, summarizes our conclusions. The formulae for calculating the rate of LFV rare decays and d_e are summarized in the appendix.

2 The model and its observable effects

In this section we specify the model and the sources of LFV and CP-violation that we are going to study.

In this paper, we consider the Minimal Supersymmetric Standard Model

with superpotential

$$W_{\text{MSSM}} = -Y_i \widehat{e}_{Ri}^c \widehat{L}_i \cdot \widehat{H}_d - \mu \widehat{H}_u \cdot \widehat{H}_d \quad (1)$$

where \widehat{L}_i , \widehat{H}_u and \widehat{H}_d are doublets of chiral superfields respectively associated with left-handed leptons and the two Higgs doublets of the MSSM. In the above formula, \widehat{e}_{Ri}^c is the chiral superfields associated with the right-handed charged lepton fields. The index “ i ” determines the flavor; $i = 1, 2, 3$ respectively correspond to e, μ, τ . Notice that we have chosen the mass basis for the charged leptons (*i.e.*, Yukawa coupling of the charged leptons is taken to be diagonal). Notice that the Yukawa terms involving the quark supermultiplets have to be added to (1). However, since we are going to concentrate on the lepton sector, we have omitted such terms. At the electroweak scale, the soft supersymmetry breaking part of the Lagrangian in general has the form

$$\begin{aligned} \mathbb{L}_{\text{soft}}^{\text{MSSM}} &= -1/2 \left(M_1 \widetilde{B}\widetilde{B} + M_2 \widetilde{W}\widetilde{W} + \text{H.c.} \right) \\ &- (A_i Y_i \delta_{ij} + A_{ij}) \widetilde{e}_{Ri}^c \widetilde{L}_j \cdot H_d + \text{H.c.} - \widetilde{L}_i^\dagger (m_{\widetilde{e}_L}^2)_{ij} \widetilde{L}_j - \widetilde{e}_{Ri}^c{}^\dagger (m_{\widetilde{e}_R}^2)_{ij} \widetilde{e}_{Rj}^c \\ &- m_{H_u}^2 H_u^\dagger H_u - m_{H_d}^2 H_d^\dagger H_d - (B_H H_u \cdot H_d + \text{H.c.}), \end{aligned} \quad (2)$$

where the “ i ” and “ j ” indices determine the flavor and \widetilde{L}_i consists of $(\widetilde{\nu}_i \widetilde{e}_{Li})$. Notice that we have divided the trilinear coupling to a flavor diagonal part ($A_i Y_i \delta_{ij}$) and a LFV part (A_{ij} with $A_{ii} = 0$). Again terms involving the squarks as well as the gluino mass term have to be added to (2). The Hermiticity of the Lagrangian implies that $m_{H_u}^2$, $m_{H_d}^2$ and the diagonal elements of $m_{\widetilde{e}_L}^2$ and $m_{\widetilde{e}_R}^2$ are all real. Moreover, without loss of generality we can rephrase the fields to make the parameters M_2 , B_H as well as Y_i real. In such a basis, the rest of above parameters can in general be complex and can be considered as sources of CP-violation giving contributions to EDMs.

After electroweak symmetry breaking, the A -terms in (2) as well as the terms in superpotential induce left-right mixing. The Hermitian 6×6 mass

matrix of $(\tilde{e}_R)_i$ and $(\tilde{e}_L)_j$ can in general be written in terms of three 3×3 mass sub-matrices m_L^2 , m_R^2 and m_{LR}^2 as follows

$$L_{\text{lepton}} = - \begin{pmatrix} \tilde{e}_L^\dagger & \tilde{e}_R^\dagger \end{pmatrix} \begin{pmatrix} m_L^2 & m_{LR}^{2\dagger} \\ m_{LR}^2 & m_R^2 \end{pmatrix} \begin{pmatrix} \tilde{e}_L \\ \tilde{e}_R \end{pmatrix}. \quad (3)$$

The formulae for m_L^2 , m_R^2 and m_{LR}^2 in terms of the soft supersymmetry breaking potential are given in Eqs. (12,13,14) of the appendix. With above Lagrangian and superpotential, the LF is conserved if and only if $A_{ij} = 0$ and the off-diagonal elements of $m_{\tilde{e}_L}^2$ and $m_{\tilde{e}_R}^2$ vanish (for $i \neq j$, $(m_L^2)_{ij} = (m_R^2)_{ij} = A_{ij} = 0$). At the one loop level, in the lepton conserving case, each A term can contribute to the EDM of only the corresponding fermion. For example, at the one loop level, the phase of A_τ will have no effect on d_e but can induce an EDM for the tau lepton of order of $\text{Im}(A_\tau)m_\tau/m_{\text{SUSY}}^3$. Considering the fact that the bound on the EDM of tau is much weaker than this [13], no bound on ϕ_{A_τ} from d_τ can be derived. In the LF conserving case, d_e will receive significant contributions from the phases of A_e , μ and M_1 . Thus, the strong bound on d_e can be translated into bounds on the phases of these parameters. In the literature, it is shown that for relatively low scale supersymmetry ($m_{\text{SUSY}} < 500$ GeV), the bounds on these phases from d_e are very strong [8] unless severe cancelation takes place [6].

At the two-loop level, even in the lepton flavor conserving case, the phase of A_τ can induce a contribution to d_e as well as to d_n [14]¹. For relatively large values of $\tan\beta$ ($\tan\beta \geq 10$) and $m_{\text{SUSY}} \simeq 100$ GeV, the bound on d_e can be translated into a bound of order of few hundred GeV on $\text{Im}[A_\tau]$. The limit from the bound on d_n even is less stringent ².

For LFV case, the A -term associated with a definite lepton flavor can in principle affect the EDM of a lepton of another flavor, even at the one-loop

¹Although in [14] the two-loop effects of only $\text{Im}[A_b]$ and $\text{Im}[A_t]$ on d_e and d_n have been discussed, similar discussion also holds for $\text{Im}[A_\tau]$.

²We would like to thank the anonymous referee for pointing out such a possibility.

level. In particular if the $e\tau$ element of m_L^2 and m_R^2 or A_{ij} are nonzero, the phase of A_τ can induce an EDM for the electron exceeding the present bound by several orders of magnitudes. As a result, in this case the strong bound on d_e can severely restrict the phase of A_τ . In order to study this bound, we have to first consider the bounds on the LFV masses and A -terms from the bounds on the LFV decay modes of the charged leptons. Notice that throughout this paper we have implicitly assumed that the origin of LFV lies at an energy scale far above the scale of the electroweak symmetry breaking. We therefore have the same LFV-violating elements for the left-handed charged lepton and sneutrino mass matrices.

The strongest upper bound on the LFV elements of the slepton mass matrices comes from the following experimental bound:

$$\text{Br}(\mu \rightarrow e\gamma) < 1.2 \times 10^{-11} \quad (4)$$

which for $m_{\text{SUSY}} \sim 100$ GeV implies $(m_L^2)_{e\mu}, (m_R^2)_{e\mu} \lesssim 10^{-4} - 10^{-3}(m_{\text{SUSY}}^2)$ and $A_{e\mu}, A_{\mu e} \lesssim 0.05 m_{\text{SUSY}}^2 / \langle H_d \rangle$. Throughout this paper we will set these LFV elements equal to zero:

$$(m_L^2)_{e\mu} = (m_R^2)_{e\mu} = 0 \quad \text{and} \quad A_{e\mu} = A_{\mu e} = 0.$$

There are also strong bounds on the branching ratios of LFV decay modes of the tau lepton:

$$\text{Br}(\tau \rightarrow e\gamma) < 9.4 \times 10^{-8} \quad [15] \quad (5)$$

and

$$\text{Br}(\tau \rightarrow \mu\gamma) < 1.6 \times 10^{-8} \quad [15] \quad (6)$$

which can be respectively translated into bounds on the τe - and $\tau\mu$ -elements. However, it can be shown that the bound on the τe -elements from (5) are not very strong and these elements can be of the same order as the diagonal elements. Suppose that both the τe - and $\tau\mu$ -elements are nonzero. This

means the e - and μ -lepton numbers are both violated and the $\mu \rightarrow e\gamma$ decay can therefore take place despite the vanishing μe -elements. In fact, for relatively large τe -elements saturating the bound from (5), the bound (4) can be translated into a strong bound on the $\tau\mu$ -elements which is more stringent than the bound from $\text{Br}(\tau \rightarrow \mu\gamma)$. Throughout this paper, we will set all the $\tau\mu$ equal to zero:

$$(m_L^2)_{\mu\tau} = (m_R^2)_{\mu\tau} = 0 \quad \text{and} \quad A_{\mu\tau} = A_{\tau\mu} = 0.$$

In this scenario, the μ -flavor number is thus conserved.

As shown in the literature, integrating out the heavy supersymmetric states, $\tau \rightarrow e\gamma$ can be described by the following effective Lagrangian

$$e\epsilon_\alpha^\dagger m_\tau q_\beta [\bar{e}_R \sigma^{\alpha\beta} (A_L)_{e\tau} \tau_L + \bar{e}_L \sigma^{\alpha\beta} (A_R)_{e\tau} \tau_R] + \text{H.c.} \quad (7)$$

where ϵ_α is the photon field and q_β is its four-momentum and $\sigma^{\alpha\beta} = \frac{i}{2}[\gamma^\alpha, \gamma^\beta]$. The formulae for A_L and A_R in terms of the supersymmetric parameters have been derived in [16] for the CP-invariant case. We have re-derived the formulae for the CP-violating case. The results can be found in the appendix. Our results are in agreement with [16] in the CP-invariant limit. Using (7) it is straightforward to show that in the rest frame of the tau lepton, the partial decay rate is given by

$$\frac{d\Gamma(\tau \rightarrow e\gamma)}{d\cos\theta} = \frac{e^2}{32\pi} m_\tau^5 [|(A_L)_{e\tau}|^2(1 + \cos\theta) + |(A_R)_{e\tau}|^2(1 - \cos\theta)] \quad (8)$$

where θ is the angle between the spin of the tau and the momentum of the emitted electron. Integrating over θ we obtain

$$\Gamma(\tau \rightarrow e\gamma) = \frac{e^2}{16\pi} m_\tau^5 (|(A_L)_{e\tau}|^2 + |(A_R)_{e\tau}|^2). \quad (9)$$

Notice that different sets of LFV mass matrix elements can result in the same rate for $\tau \rightarrow e\gamma$. Let us define the A_P asymmetry as follows

$$A_P = 4 \times \frac{\int_0^1 \frac{d\Gamma(\tau \rightarrow e\gamma)}{d\cos\theta} d\cos\theta - \int_{-1}^0 \frac{d\Gamma(\tau \rightarrow e\gamma)}{d\cos\theta} d\cos\theta}{\Gamma(\tau \rightarrow e\gamma)}. \quad (10)$$

Using (8), we can prove that

$$A_P = \frac{|(A_L)_{e\tau}|^2 - |(A_R)_{e\tau}|^2}{|(A_L)_{e\tau}|^2 + |(A_R)_{e\tau}|^2}.$$

Thus by measuring the partial decay rate of τ , we will be able to extract not only $(|(A_L)_{e\tau}|^2 + |(A_R)_{e\tau}|^2)$ but also $(|(A_L)_{e\tau}|^2 - |(A_R)_{e\tau}|^2)$. In [17], it has been shown that by studying the angular distributions of the final particles at an e^-e^+ collider such as a B-factory, it will be possible to derive A_P . A_P provides us with more information on the LFV parameters of the underlying theory. For example, if the source of LFV is a canonical seesaw mechanism embedded in the MSSM, we expect $(m_R^2)_{e\tau} \ll (m_L^2)_{e\tau}$ and $A_{e\tau} \ll A_{\tau e}$ which means $|(A_L)_{e\tau}|^2 \ll |(A_R)_{e\tau}|^2$ and therefore $A_P \rightarrow -1$. In this paper, we will study the correlation between d_e , $\text{Br}(\tau \rightarrow e\gamma)$ and A_P and discuss the possibility of resolving the degeneracies by combining the information on their values.

3 New contributions to d_e in the presence of LFV

Let us for the moment suppose $A_{e\tau} = A_{\tau e} = 0$. As illustrated in Fig. 1, for nonzero $(m_R^2)_{e\tau}$ and $(m_L^2)_{\tau e}$, the phase of A_τ can induce a contribution to d_e . As a result for definite values of the off-diagonal mass elements, the bound on d_e can be interpreted as a bound on ϕ_{A_τ} or on $\text{Im}(A_\tau)$. Consider the case that both $(m_R^2)_{\tau e}$ and $(m_L^2)_{\tau e}$ are close to the corresponding bounds from $\text{Br}(\tau \rightarrow e\gamma)$. In this case, $\text{Br}(\tau \rightarrow e\gamma)$ is close to its present bound and A_P takes a value in the interval $(-1,1)$; *i.e.*, $A_P \neq \pm 1$. For such a configuration, we expect the bound on $\text{Im}(A_\tau)$ to be more stringent than the bound on $\text{Im}(A_e)$ because the effect of $\text{Im}(A_\tau)$ is given by $m_\tau \text{Im}(A_\tau) (m_R^2)_{e\tau} (m_L^2)_{e\tau} / m_{\text{susy}}^7$, whereas the effect of $\text{Im}(A_e)$ is proportional to $m_e \text{Im}(A_e) / m_{\text{susy}}^3$. Now, suppose only one of $(m_R^2)_{e\tau}$ and $(m_L^2)_{\tau e}$ is close to its upper bound from $\text{Br}(\tau \rightarrow e\gamma)$ and the

other is zero or very small. In this case, A_P will converge either to 1 (for $(m_R^2)_{e\tau} \gg (m_L^2)_{e\tau}$) or to -1 (for $(m_L^2)_{e\tau} \gg (m_R^2)_{e\tau}$). From Fig. 1 we observe that if only one of $(m_R^2)_{e\tau}$ or $(m_L^2)_{\tau e}$ is nonzero and the rest of the $e\tau$ entries (including $A_{e\tau}$ and $A_{\tau e}$) vanish, at one-loop level, the phase of A_τ cannot contribute to d_e .

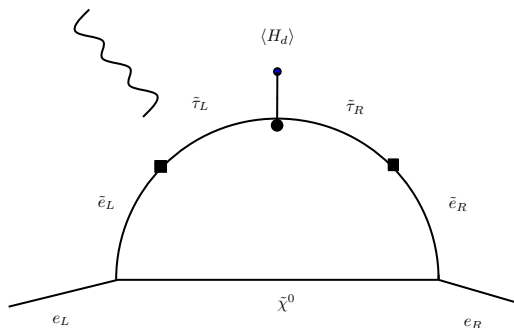


Figure 1: A neutralino exchange diagram contributing to d_e . The photon can attach to any of the \tilde{e}_L , $\tilde{\tau}_L$, $\tilde{\tau}_R$ or \tilde{e}_R propagators. The boxes on the left and right sides respectively depict insertion of $(m_L^2)_{e\tau}$ and $(m_R^2)_{e\tau}$. The circles indicate insertion of the A_τ vertex and the vacuum expectation value of H_d .

Figs. 2-4 demonstrate this observation. To draw the figures in this paper, we have chosen the mass spectrum corresponding to the α benchmark proposed in [18]. However, we have allowed the mass spectrum of the staus to slightly deviate from these benchmarks. Notice that at these benchmarks, the lightest stau is considerably heavier than the lightest neutralino so stau-neutralino coannihilation cannot play any significant role in fixing the dark matter relic density. As a result, a slight change of stau parameters will not dramatically affect the cosmological predictions. Although for illustrative purposes we have displayed the mass insertion approximation in Fig. 1, to

calculate d_e and $\text{Br}(\tau \rightarrow e\gamma)$ we have used the exact formulae (without the mass insertion approximation) presented in the appendix.

Fig. 2 depicts d_e in terms of the sine of ϕ_{A_τ} for $A_{ij} = 0$ and various values of $(m_L^2)_{e\tau}$ and $(m_R^2)_{e\tau}$. This diagram demonstrates that for $(m_L^2)_{e\tau}$ and $(m_R^2)_{e\tau}$ close to their bounds from $\text{Br}(\tau \rightarrow e\gamma)$, a very strong bound on ϕ_{A_τ} can be derived. That is while if there is a hierarchy between these elements, the bound will be much weaker. Notice that for the input parameters chosen for this figure, $\text{Br}(\tau \rightarrow e\gamma)$ lies close to its present bound: $10^{-8} < \text{Br}(\tau \rightarrow e\gamma) < 10^{-7}$.

Fig. 3 demonstrates the correlation between A_P and d_e . As explained in the caption, the input mass spectrum is that of the α benchmark [18] and $|A_\tau| = 500$ GeV. We have set $A_{e\tau}$ and $A_{\tau e}$ equal to zero and the maximal value for the CP-violating phase is chosen: $\phi_{A_\tau} = \pi/2$. $(m_L^2)_{\tau e}$ and $(m_R^2)_{\tau e}$ pick up random values at a logarithmic scales. Points for which $\text{Br}(\tau \rightarrow e\gamma)$ exceeds its present bound are eliminated. Fig. (3-a) shows us that if $\phi_{A_\tau} = \pi/2$, d_e for a significant portion of the scatter points exceeds the present bound. Fig. (3-b) shows A_P versus $\text{Br}(\tau \rightarrow e\gamma)$ for the same scatter points. To illustrate the correlation between A_p and d_e , we have shown the corresponding scatter points in Fig 3-a and Fig 3-b with the same color and symbol. That is at points marked with green dots, d_e exceeds its present bound and at the scatter points marked with blue cross “ \times ” $10^{-29} < d_e < 1.4 \times 10^{-27} e$ cm. The scatter points depicted by pink circle, which appear in Fig. (3-b) as two pink horizontal lines at $A_P = \pm 1$, correspond to $d_e < 10^{-29} e$ cm. From Fig. (3-b) we conclude that for $A_{e\tau} = A_{\tau e} = 0$, the bound on d_e can be satisfied if either $\text{Br}(\tau \rightarrow e\gamma)$ is very small (which means that all the LFV masses are very small) or A_P is close to ± 1 (meaning that there is a hierarchy between the LFV elements). In other words within this scenario, if future searches find $5 \times 10^{-10} < \text{Br}(\tau \rightarrow e\gamma)$ and $-0.9 < A_P < 0.9$, the bound on d_e should be interpreted either as a bound on ϕ_{A_τ} or as an

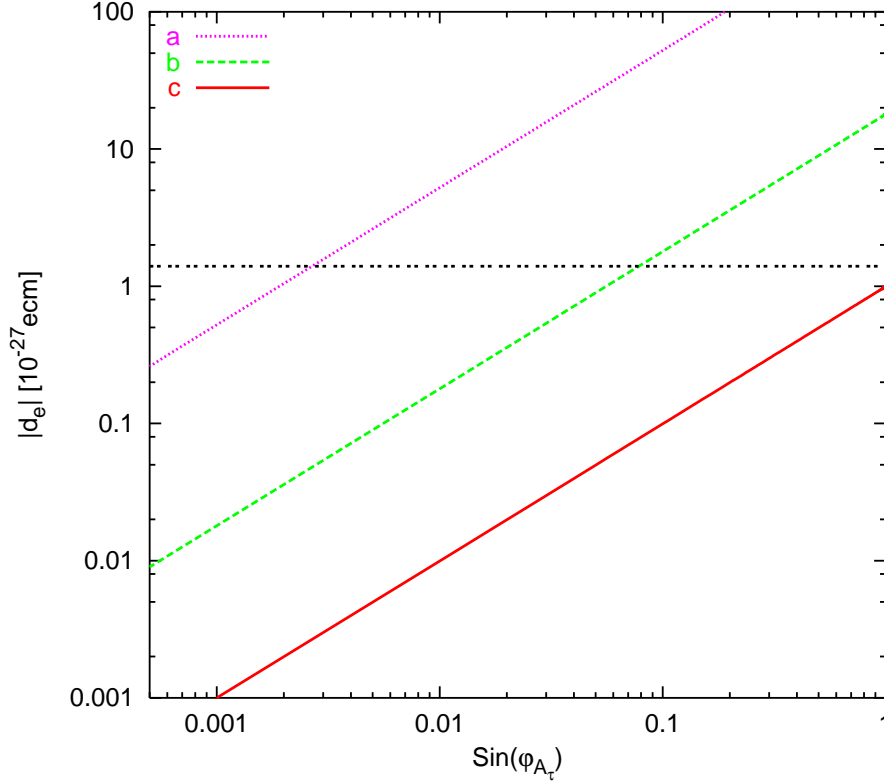


Figure 2: d_e versus $\sin \phi_{A_\tau}$. The input parameters correspond to the α benchmark proposed in [18]: $|\mu| = 375$ GeV, $m_0 = 210$ GeV, $M_{1/2} = 285$ GeV and $\tan \beta = 10$ and we have set $|A_\tau| = 500$ GeV. All the LFV elements of the slepton mass matrix are set to zero except $(m_L^2)_{e\tau}$ and $(m_R^2)_{e\tau}$. The dotted (pink) line labeled (a) corresponds to $(m_L^2)_{e\tau} = 3500$ GeV² and $(m_R^2)_{e\tau} = 15000$ GeV². The dashed (green) line labeled (b) corresponds to $(m_L^2)_{e\tau} = 50$ GeV² and $(m_R^2)_{e\tau} = 37000$ GeV². The solid (red) line labeled (c) corresponds to $(m_L^2)_{e\tau} = 3500$ GeV² and $(m_R^2)_{e\tau} = 30$ GeV². The horizontal dotted line at 1.4×10^{-27} e cm depicts the present experimental limit [13] on d_e .

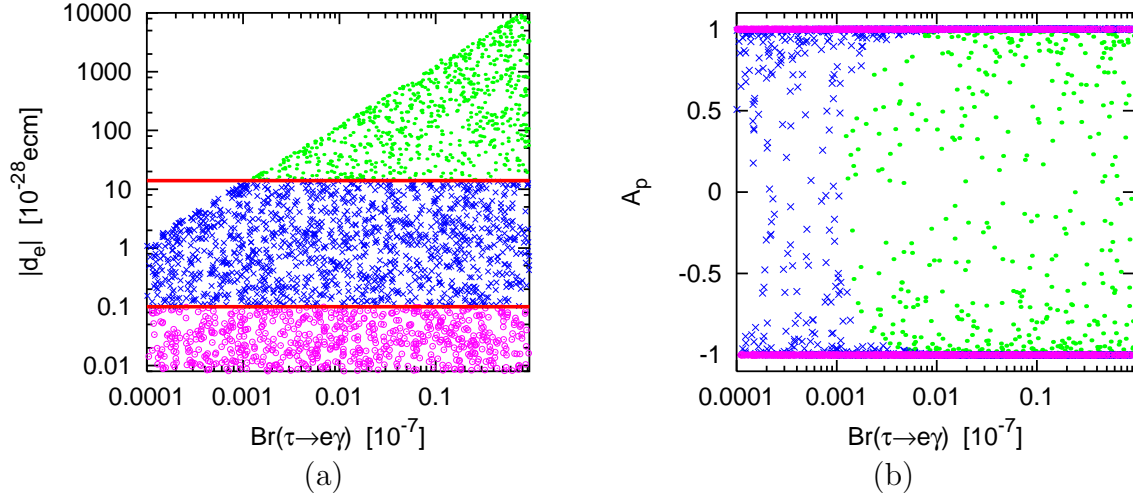


Figure 3: a) Scatter plot of d_e versus $\text{Br}(\tau \rightarrow e\gamma)$. The input parameters correspond to the α benchmark proposed in [18]: $|\mu| = 375$ GeV, $m_0 = 210$ GeV, $M_{1/2} = 285$ GeV and $\tan\beta = 10$. We have however set $\phi_{A_\tau} = \pi/2$ and $|A_\tau| = 500$ GeV. All the LFV elements of the slepton mass matrix are set to zero except $(m_L^2)_{e\tau}$ and $(m_R^2)_{e\tau}$ which pick up random values at a logarithmic scale respectively from $(5.9 \times 10^{-4} \text{ GeV}^2, 5.9 \times 10^3 \text{ GeV}^2)$ and $(3.7 \times 10^{-3} \text{ GeV}^2, 3.7 \times 10^4 \text{ GeV}^2)$. The horizontal line at $1.4 \times 10^{-27} e \text{ cm}$ depicts the present experimental limit [13] and the one at $10^{-29} e \text{ cm}$ shows the limit that can be probed in the near future [2]. b) Scatter plot of A_p versus $\text{Br}(\tau \rightarrow e\gamma)$. For each scatter point in Fig. 3-a there is a counterpart in Fig. 3-b corresponding to the same input values for the $e\tau$ elements which is shown with the same color and symbol. Notice that points shown in pink (corresponding to $d_e < 10^{-29} e \text{ cm}$) all lie on the $A_p = \pm 1$.

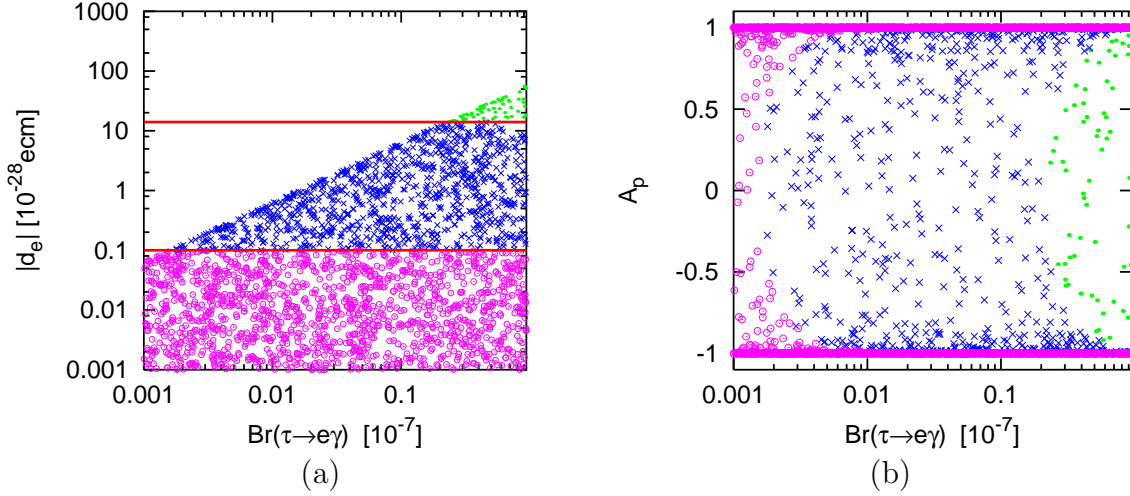


Figure 4: Similar to Fig. 3 except that $(m_L^2)_{e\tau} = (m_R^2)_{e\tau} = 0$ and instead $(m_{LR}^2)_{e\tau} (= A_{e\tau}\langle H_d \rangle)$ and $(m_{LR}^2)_{\tau e} (= A_{\tau e}\langle H_d \rangle)$ pick up random values at a logarithmic scale from $(1.2 \times 10^{-3} \text{ GeV}^2, 1.2 \times 10^3 \text{ GeV}^2)$. For each scatter point in Fig. 4-a there is a counterpart in Fig. 4-b corresponding to the same input values for the $e\tau$ elements which is shown with the same color and symbol.

indication for a cancelation between different contributions from ϕ_{A_τ} and other possible CP-violating phases. In the next section, we shall elaborate on the latter possibility in more detail. We emphasize that to draw this conclusion we have taken $A_{e\tau} = A_{\tau e} = 0$. Repeating the same analysis with different benchmarks we have found that the pattern and the correlation among $\text{Br}(\tau \rightarrow e\gamma)$, A_P and d_e are not sensitive to the input values of LF conserving parameters.

To draw Fig. 4, $(m_L^2)_{e\tau}$ and $(m_R^2)_{e\tau}$ are set equal to zero and instead

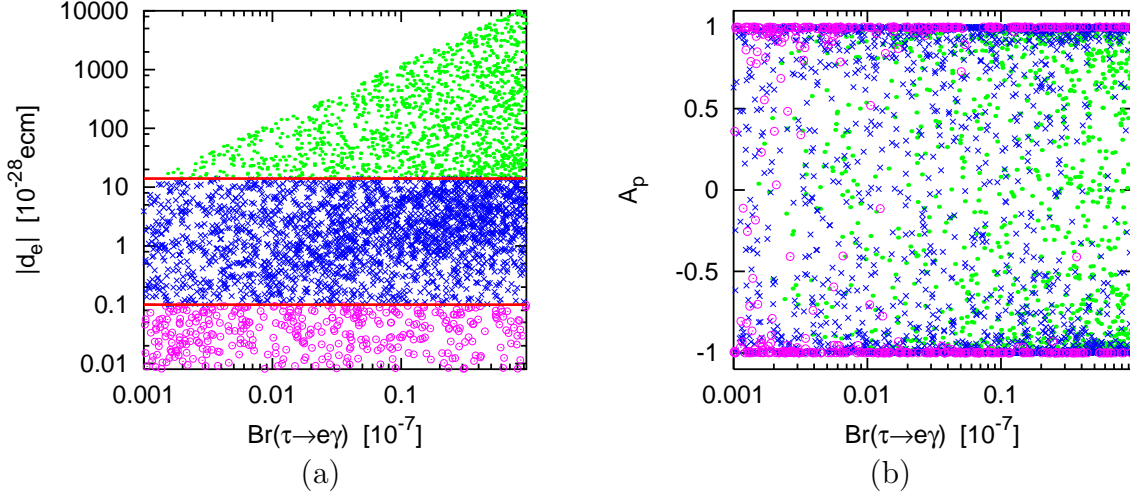


Figure 5: Similar to Fig. 3 except that here in addition to $(m_L^2)_{e\tau}$ and $(m_R^2)_{e\tau}$, $(m_{LR}^2)_{e\tau}(= A_{e\tau}\langle H_d \rangle)$ and $(m_{LR}^2)_{\tau e}(= A_{\tau e}\langle H_d \rangle)$ are allowed to be nonzero. The values of $(m_L^2)_{e\tau}$ and $(m_R^2)_{e\tau}$ are randomly chosen respectively from $(0.59 \text{ GeV}^2, 5.9 \times 10^3 \text{ GeV}^2)$ and $(3.7 \text{ GeV}^2, 3.7 \times 10^4 \text{ GeV}^2)$ at a logarithmic scale. $(m_{LR}^2)_{e\tau}$ and $(m_{LR}^2)_{\tau e}$ pick up random values at a logarithmic scale from the interval $(0.12 \text{ GeV}^2, 1.2 \times 10^3 \text{ GeV}^2)$. For each scatter point in Fig. 5-a there is a counterpart in Fig. 5-b corresponding to the same input values for the $e\tau$ elements which is shown with the same color and symbol.

random values for $A_{e\tau}$ and $A_{\tau e}$ are taken. The LF conserving parameters for Figs. (3) and (4) are the same. Like the case of Fig. (3), a significant portion of the scatter points have d_e exceeding the present bound. Moreover a similar correlation between d_e , A_P and $\text{Br}(\tau \rightarrow e\gamma)$ emerges. That is points marked with green dot (corresponding to $d_e > 1.4 \times 10^{-27} e \text{ cm}$), with blue “ \times ” (corresponding to $10^{-29} < d_e < 1.4 \times 10^{-27} e \text{ cm}$) and pink circles (corresponding to $d_e < 10^{-29} e \text{ cm}$) are scattered respectively from right to left. Notice however that in contrast to Fig. (3-b), Fig. (4-b) includes scatter points with $-0.9 < A_P < 0.9$ and $\text{Br}(\tau \rightarrow e\gamma) \sim 10^{-8}$ that satisfy the present bound on d_e (the points marked with “ \times ” in the plot). We have repeated the same analysis with the δ benchmark and have found a similar pattern. Similarity between the patterns means that the above observation does not depend on the input values for the LF conserving parameters.

In Fig. 5, the input values for the LF conserving parameters are taken to be the same as those for Figs. 3 and 4. However, $(m_L^2)_{e\tau}$, $(m_R^2)_{e\tau}$, $A_{e\tau}$ and $A_{\tau e}$ all take nonzero random values. Fig. (5-a) contains features of both Figs. (3) and (4). The significant point is that setting all the $e\tau$ mass elements nonzero, the correlation among A_P , d_e and $\text{Br}(\tau \rightarrow e\gamma)$ is lost. That is Fig. (5-b) contains points with $\text{Br}(\tau \rightarrow e\gamma) \sim 10^{-7}$, $-0.9 < A_P < 0.9$ and $d_e < 10^{-29} e \text{ cm}$. The presence of these points can be explained by the fact that when $A_{e\tau}$ and $(m_L^2)_{e\tau}$ are nonzero but $A_{\tau e} = (m_R^2)_{e\tau} = 0$ (or equivalently, when $A_{\tau e}$ and $(m_R^2)_{e\tau} \neq 0$ but $A_{e\tau} = (m_L^2)_{e\tau} = 0$) d_e , despite large ϕ_{A_τ} , remains zero but A_L can be of order of A_R which yields $-0.9 < A_P < 0.9$. As a result, without independent knowledge of the ratios of LFV elements, we cannot derive any conclusive bound on ϕ_{A_τ} even if we find $-0.9 < A_P < 0.9$ and $10^{-8} < \text{Br}(\tau \rightarrow e\gamma)$. We have repeated the same analysis for other benchmarks and the results seem to be robust against changing the mass spectrum.

As explained earlier, some models predict a certain pattern for LFV. For

example, within the framework of the seesaw mechanism embedded in the constrained MSSM, we expect the LFV to be induced mainly on the left-handed sector [19]. That is we expect $(m_R^2)_{e\tau} \ll (m_L^2)_{e\tau}$ and $A_{e\tau}/A_{\tau e} \sim m_e/m_\tau \ll 1$. This model predicts $A_P = -1$. On the contrary, within the supersymmetric SU(5) GUT model without right-handed neutrinos, the LFV is induced only on the right-handed sector [20] which implies $A_P = 1$. For both of these cases, d_e induced by ϕ_{A_τ} is negligible.

In the above discussion, we have used the bound on ϕ_{A_τ} and on $\text{Im}(A_\tau)$ interchangeably. To clarify the relation between these two, Fig. (6) has been presented which shows curves of $d_e = 1.4 \times 10^{-27} e \text{ cm}$ (the present bound) for the α and δ benchmarks and various values of the off-diagonal elements. The values of the LFV elements are chosen in a range to obtain $\text{Br}(\tau \rightarrow e\gamma)$ close to the present bound; *i.e.*, $10^{-8} < \text{Br}(\tau \rightarrow e\gamma) < 10^{-7}$. Each curve can be considered as the upper bound on ϕ_{A_τ} . These figures also confirm that when there is a hierarchy between the left and right LFV elements, the bounds are weaker. As expected, the curves have a shape close $\text{Im}(A_\tau) = |A_\tau| \sin \phi_{A_\tau} = \text{cte}$.

In summary, within a model that $A_{ij} = 0$, if $\text{Br}(\tau \rightarrow e\gamma)$ turns out to be close to its present bound and A_P deviates from +1 and -1, the bound on d_e puts a strong bound on $\text{Im}(A_\tau)$. However, if $A_P = \pm 1$, the bound on d_e can be explained by a hierarchy between the $(m_L^2)_{\tau e}$ and $(m_R^2)_{\tau e}$ elements instead of by the smallness of $\text{Im}(A_\tau)$. Similar discussion holds for the scenario in which $(m_R^2)_{e\tau} = (m_L^2)_{e\tau} = 0$ and instead $A_{e\tau}$ and $A_{\tau e}$ are nonzero: while for $A_P \neq \pm 1$, the bound on d_e can severely restrict ϕ_{A_τ} , for $A_P = \pm 1$ we cannot obtain any bound on ϕ_{A_τ} from d_e . However, within a scenario that $A_{e\tau}$, $A_{\tau e}$, $(m_R^2)_{\tau e}$ and $(m_L^2)_{\tau e}$ are all large, we cannot derive any bound on ϕ_{A_τ} even if $A_P \neq \pm 1$. Thus, in order to derive a conclusive bound on ϕ_{A_τ} , one has to resolve these degeneracies seeking help from an experiment other than the rare τ decay. Studying LFV signals at a e^-e^+ collider with energy of center

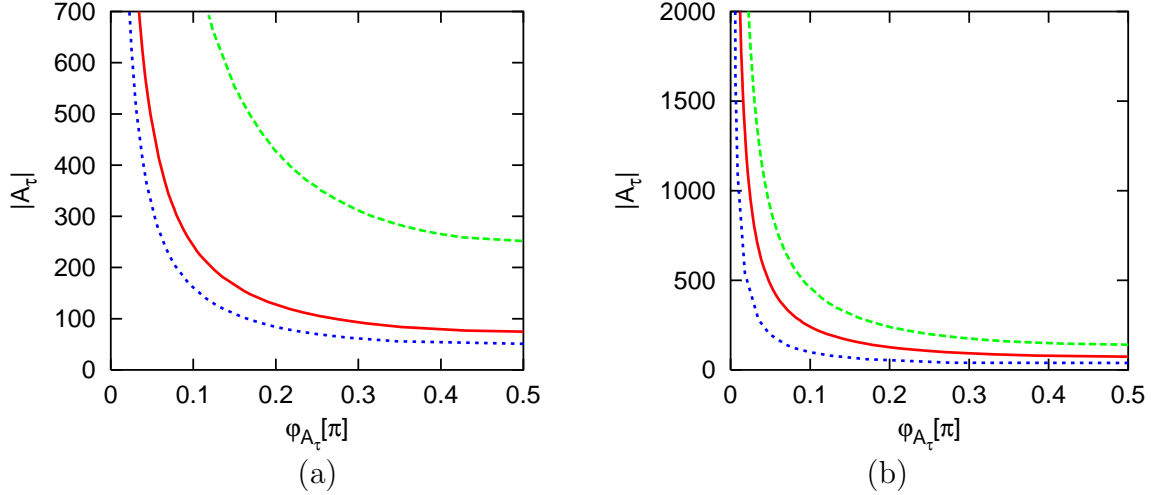


Figure 6: Contour plots for $d_e = 1.4 \times 10^{-27}$. a) The α benchmark proposed in [18] is taken as the input. The dotted blue curve corresponds to $(m_L^2)_{e\tau} = 3500 \text{ GeV}^2$, $(m_R^2)_{e\tau} = 1500 \text{ GeV}^2$ and $(m_{LR}^2)_{\tau e} = (m_{LR}^2)_{e\tau} = 0$ and the thick solid red curve corresponds to $(m_L^2)_{e\tau} = 3000 \text{ GeV}^2$, $(m_R^2)_{e\tau} = 1000 \text{ GeV}^2$, $(m_{LR}^2)_{e\tau} = 300 \text{ GeV}^2$ and $(m_{LR}^2)_{\tau e} = 100 \text{ GeV}^2$. The dashed green curve corresponds to $(m_L^2)_{e\tau} = 3000 \text{ GeV}^2$, $(m_R^2)_{e\tau} = 100 \text{ GeV}^2$, $(m_{LR}^2)_{e\tau} = 10 \text{ GeV}^2$ and $(m_{LR}^2)_{\tau e} = 500 \text{ GeV}^2$. b) The δ benchmark proposed in [18] is taken as the input: $|\mu| = 920 \text{ GeV}$, $m_0 = 500 \text{ GeV}$, $M_{1/2} = 750 \text{ GeV}$ and $\tan \beta = 10$. The dotted blue curve corresponds to $(m_L^2)_{e\tau} = 7 \times 10^4 \text{ GeV}^2$ and $(m_R^2)_{e\tau} = 2 \times 10^4 \text{ GeV}^2$ and the thick red curve corresponds to $(m_L^2)_{e\tau} = 2 \times 10^4 \text{ GeV}^2$, $(m_R^2)_{e\tau} = 3 \times 10^4 \text{ GeV}^2$, $(m_{LR}^2)_{e\tau} = 3000 \text{ GeV}^2$ and $(m_{LR}^2)_{\tau e} = 7000 \text{ GeV}^2$. The dashed green curve corresponds to $(m_L^2)_{e\tau} = 1 \times 10^5 \text{ GeV}^2$, $(m_R^2)_{e\tau} = 3000 \text{ GeV}^2$, $(m_{LR}^2)_{e\tau} = 30 \text{ GeV}^2$ and $(m_{LR}^2)_{\tau e} = 8000 \text{ GeV}^2$.

of mass of a few hundred GeV can help in this direction [21]. In this paper we have concentrated on the possibilities that the ongoing experiments can bring about. Studying the possibilities with ILC is beyond the scope of the present paper.

4 Degeneracies between different sources of CP-violation

In the previous section, we had assumed that the only source of CP-violation is the phase of A_τ . However, within the framework of general MSSM, there are multiple sources of CP-violation. In the basis described in Sec. 2, these phases include the phases of A_e , the μ -term and M_1 (the Bino mass) that can contribute to d_e regardless of the conservation or violation of LF. Within the scenario considered in this paper, in addition to these sources, the phases of $A_{e\tau}$, $A_{\tau e}$, $(m_L^2)_{e\tau}$ and $(m_R^2)_{e\tau}$ can be also considered as independent sources of CP-violation that can contribute to d_e . If we assume that only one of these various phases is nonzero, the present bound on d_e can be interpreted as a strong bound on the nonzero phase. However, in general when more than one phase is present, the effects of different phases can cancel each other [6]. Moreover, if the forthcoming searches report a nonzero d_e , without additional information, we cannot disentangle the source of CP-violation. In this section, we discuss the degeneracies between different sources of CP-violation with special emphasis on the possibility of cancelation.

Figs. (7-9) display the degeneracies between possible CP-violating phases. To draw these figures, we have inserted the mass spectrum of the α benchmark proposed in [18] (see caption of Fig. 3 for the values of the relevant parameters) and we have set $A_\tau = A_e = 500$ GeV. Each of Figs. (7-9) corresponds to a different set of absolute values for the LFV elements $(m_L^2)_{e\tau}$, $(m_R^2)_{e\tau}$, $A_{\tau e}$ and $A_{e\tau}$. Each curve in these figures shows d_e versus $\text{Br}(\tau \rightarrow e\gamma)$

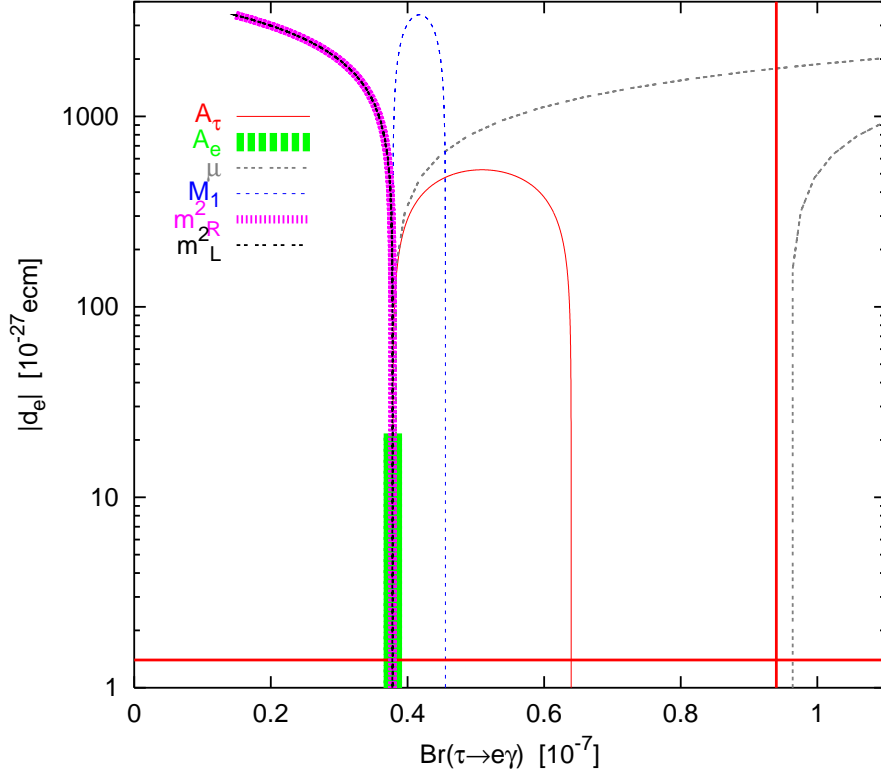


Figure 7: d_e versus $\text{Br}(\tau \rightarrow e\gamma)$ as the CP-violating phases vary between zero and π . The input parameters correspond to the α benchmark proposed in [18]: $|\mu| = 375$ GeV, $m_0 = 210$ GeV, $M_{1/2} = 285$ GeV and $\tan\beta = 10$ and we have set $A_\tau = A_e = 500$ GeV. All the LFV elements of the slepton mass matrix are set zero except that $|(m_L^2)_{e\tau}| = 3500$ GeV² and $|(m_R^2)_{e\tau}| = 15000$ GeV². To draw the curves all phases are set zero except one that varies between 0 and π . As illustrated in the legend of the figure, the thin solid red curve, dotted grey curve and light blue dashed curve respectively correspond to varying phases of A_τ , μ and M_1 . The thin black and thick pink dotted curves correspond to the phases of $(m_L^2)_{e\tau}$ and $(m_R^2)_{e\tau}$ which for $A_{e\tau} = A_{\tau e}$ lie over each other. The thick green vertical line stretching up to $d_e = 2 \times 10^{-26}$ e cm depicts the effect of the phase of A_e . The horizontal line at 1.4×10^{-27} e cm depicts the present experimental limit [13] and the vertical line shows the present experimental bound on $\text{Br}(\tau \rightarrow e\gamma)$ at 9.4×10^{-8} [15].

as a certain CP-violating phase varies from zero to π while the rest of the phases are set to zero. As expected all the curves converge at $d_e = 0$ which corresponds to the zero value of the varying phase. As the value of the varying phase reaches $\pi/2$, d_e obtains its maximum value so the peak of each curve corresponds to the varying phase equal to $\pi/2$. The horizontal lines at $d_e = 1.4 \times 10^{-27} e$ cm in the figures show the present upper bound on d_e and the vertical lines at $\text{Br}(\tau \rightarrow e\gamma) = 9.4 \times 10^{-8}$ show the present bound on $\text{Br}(\tau \rightarrow e\gamma)$. In the following, we discuss these figures one by one.

Drawing Fig. 7, we have set $|(m_L^2)_{e\tau}| = 3500 \text{ GeV}^2$, $|(m_R^2)_{e\tau}| = 15000 \text{ GeV}^2$ and $A_{e\tau} = A_{\tau e} = 0$. The CP-violating phases that can contribute to d_e include ϕ_{A_e} , ϕ_{A_τ} , ϕ_μ , ϕ_{M_1} and the phases of $(m_L^2)_{e\tau}$ and $(m_R^2)_{e\tau}$. The thick vertical line at $\text{Br}(\tau \rightarrow e\gamma) = 3.8 \times 10^{-8}$ corresponds to the variation of ϕ_{A_e} in $[0, \pi]$. This line shows that $\text{Br}(\tau \rightarrow e\gamma)$ does not significantly change as ϕ_{A_e} varies. The reason is that the effect of A_e on $\text{Br}(\tau \rightarrow e\gamma)$ is much smaller than the dominant effect. The line associated with ϕ_{A_e} (the thick line) reaches values of d_e up to one order of magnitude higher than the present bound on d_e which means if ϕ_{A_e} is the only contributor to d_e , it cannot be larger than $\mathcal{O}(0.1)$. This bound is similar to the bound in the LF conserving case. Notice that the effects of the rest of phases can exceed the maximal contribution from ϕ_{A_e} by more than one order of magnitude. In this figure, the curves associated with the phases of $(m_L^2)_{e\tau}$ and $(m_R^2)_{e\tau}$, which are depicted by black and pink dotted curves, coincide. This observation is valid as long as $A_{e\tau} = A_{\tau e} = 0$ because the diagram shown in Fig. 1 – which in this case is the only diagram contributing to d_e – is sensitive only to the relative phase of $(m_L^2)_{e\tau}$ and $(m_R^2)_{e\tau}$. Another peculiar feature of Fig. (7) is that the contribution of ϕ_{M_1} to d_e can exceed the maximum d_e from ϕ_μ . This is opposite to the LF conserving case in which the effect of ϕ_μ is larger because, while ϕ_{M_1} can induce d_e only through the subdominant neutralino-exchange diagram, ϕ_μ can induce EDM also through the dominant chargino-exchange

diagram. In contrast to the LF conserving case, in the case of Fig. (7) the neutralino exchange diagram dominates because as explained in the previous section, once we turn on the $e\tau$ elements, the neutralino-exchange diagram contributing to d_e is enhanced by a factor of m_τ/m_e . As a result, the effect of ϕ_{M_1} is enhanced.

Now let us discuss the degeneracy and the possibility of cancellation among different contributions. Replacing a phase with its opposite value, its contribution to d_e will change sign. As a result if we find two phases whose contributions to $|d_e|$ have the same values, we can conclude that cancellation can take place for at least one pair of values. Fig. 7 shows that the curve associated with ϕ_{A_e} has a complete overlap with the low phase part of the other curves. That is for any value of ϕ_{A_e} , there is a value for other phases which can mimic the effect of ϕ_{A_e} . Thus, if the future EDM searches report a nonzero value for d_e , there will be an ambiguity in interpretation of the observation in terms of the phases. Cancellation is another consequence of this overlap. This figure shows that turning on more than one nonzero phase, cancellation can make even the maximal value of ϕ_{A_e} consistent with the present bound on d_e . That is the contribution of $\phi_{A_e} = \pi/2$ can be canceled out by the effect(s) of any of the phases ϕ_{M_1} , ϕ_μ or the phases of $(m_L^2)_{e\tau}$ and $(m_R^2)_{e\tau}$ if these phases are $\simeq \pi/500$. The contribution of $\phi_{A_e} = \pm\pi/2$ can be also canceled out by the contribution of ϕ_{A_τ} if $|\phi_{A_\tau}| \simeq \pi/80$.

Whereas the phase of A_e can only show up in d_e , the rest of phases can manifest themselves as CP-odd effects at ILC [11]. Moreover, ϕ_{M_1} and ϕ_μ can give a detectable contribution to the EDM of the neutron [22], mercury [23] and deuteron [24] through inducing chromoelectric dipole moments and EDMs to the light quarks. Thus, from the experimental point of view, cancellation between the effects of these phases is more exciting as it can open up the possibility of large phases and therefore CP-odd observable quantities in experiments other than d_e searches. Fig. 7 shows that there are values

of ϕ_{M_1} and/or the phases of $(m_L^2)_{e\tau}$ and/or $(m_R^2)_{e\tau}$ whose contribution to d_e can cancel even the maximal effect from ϕ_μ . That is even $\phi_\mu = \pm\pi/2$ is consistent with the bound on d_e but in order to cancel the effects down to the present bound a fine-tuning better than 0.1% is needed. In [9], it was also shown that turning on the LFV elements of mass matrix, the effect of ϕ_μ on d_e can be canceled by the effects of the phases of the off-diagonal elements. This result is obviously sensitive to the largeness of the absolute values of the LFV elements which are constrained by the null results of searches for the LFV rare lepton decays. Bearing in mind that since [9], these bounds have significantly improved the above discussion can be considered as an update and re-confirmation of the claim in [9] in view of the recent bounds. Notice however that a large ϕ_μ can also give contributions to d_n and d_{Hg} exceeding their present bounds. The correlation between d_e and d_{Hg} has been systematically studied in [25]. To satisfy the bounds on d_n and d_{Hg} in the presence of a large ϕ_μ , there should be another cancelation scenario at work in the quark sector. This further suppresses the allowed parameter space; *i.e.*, a *double-folded* fine-tuning.

Let us now suppose that there is a symmetry or a mechanism that sets $\phi_\mu = \phi_{M_1} = 0$ so the bounds on d_n and d_{Hg} are naturally satisfied without the above mentioned *double-folded* fine-tuning problem. Let us also suppose that ϕ_{A_τ} and the phases of $(m_L^2)_{e\tau}$ and $(m_R^2)_{e\tau}$ are large. Fig. 7 shows that this scenario is not ruled out by the d_e bound because there is still the possibility of cancelation between the contributions of the nonzero phases. To cancel the effects of $\phi_{A_\tau} \simeq \pi/2$ on d_e down to the present bound, a fine-tuning better than 1% is required.

Fig. (8) has an input similar to that of Fig. (7) except that $A_{e\tau}$ and $A_{\tau e}$ are set nonzero and smaller values for $(m_L^2)_{e\tau}$ and $(m_R^2)_{e\tau}$ are chosen. Notice that unlike Fig. (7) curves associated with the phases of $(m_L^2)_{e\tau}$ and $(m_R^2)_{e\tau}$ split. The peak of the ϕ_{A_τ} curve in Fig. (8) lies one order of magnitude below

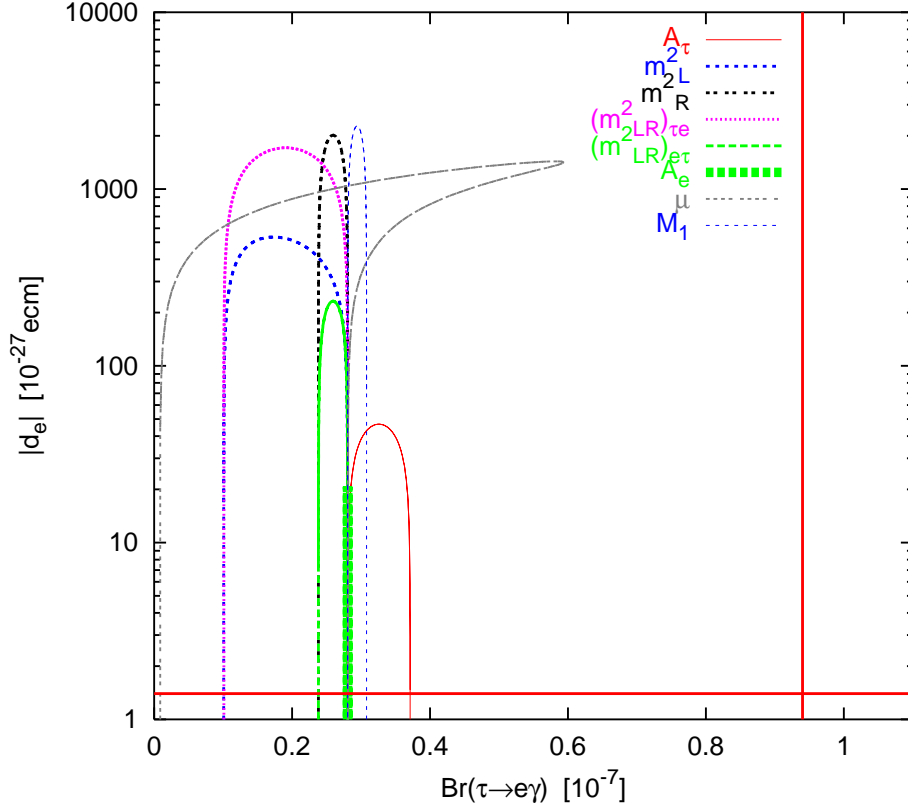


Figure 8: Similarly to Fig. 7 except that here we have set $|(m_L^2)_{e\tau}| = 1000 \text{ GeV}^2$, $|(m_R^2)_{e\tau}| = 5000 \text{ GeV}^2$ and $|(m_{LR}^2)_{e\tau}| = |(m_{LR}^2)_{\tau e}| = 300 \text{ GeV}^2$. The thin solid red curve, light dash-dotted grey curve, light blue dashed curve, solid dashed dark blue curve and thick black dotted curve respectively correspond to the varying phase of A_τ , μ , M_1 , $(m_L^2)_{e\tau}$ and $(m_R^2)_{e\tau}$. The thick green vertical line stretching up to $d_e = 2.1 \times 10^{-26} e \text{ cm}$ depicts the effect of the phase of A_e . The light pink curve and thin green curve respectively correspond to phases of $(m_{LR}^2)_{\tau e}$ and $(m_{LR}^2)_{e\tau}$. The horizontal line at $1.4 \times 10^{-27} e \text{ cm}$ depicts the present experimental limit [13] and the vertical line at 9.4×10^{-8} shows the present experimental bound on $\text{Br}(\tau \rightarrow e\gamma)$ [15].

that in Fig. (7). That is because the absolute values of $(m_L^2)_{e\tau}$ and $(m_R^2)_{e\tau}$ in Fig. (8) are smaller. Had we set these elements larger, the effect of ϕ_{A_τ} on d_e would have been larger but also the value of $\text{Br}(\tau \rightarrow e\gamma)$ would have increased. The rest of the argument for Fig. (7) holds for Fig. (8), too.

Fig. (9) displays the dependence of d_e and $\text{Br}(\tau \rightarrow e\gamma)$ on different phases for the case that there is a hierarchy between the left and right LFV elements: $|A_{e\tau}| \ll |A_{\tau e}|$ and $|(m_R^2)_{e\tau}| \ll |(m_L^2)_{e\tau}|$. Because of this hierarchy, the effect of ϕ_{A_τ} on d_e has dropped below the present bound which is expected following the discussion in the previous section. The lines associated with the phases of $(m_R^2)_{e\tau}$ and $(m_{LR}^2)_{e\tau}$ appear as vertical lines which means $\text{Br}(\tau \rightarrow e\gamma)$ does not depend on these phases. This is expected because $|(m_R^2)_{e\tau}|$ and $|(m_{LR}^2)_{e\tau}|$ are very small. However, the effects of their phases can still exceed the present bounds. The figure also shows that $\text{Br}(\tau \rightarrow e\gamma)$ strongly depends on the phases of $(m_L^2)_{e\tau}$ and $(m_{LR}^2)_{\tau e}$. The effect of ϕ_{A_e} is similar to the previous cases. The ϕ_{M_1} curve also appears as a vertical line which means $\text{Br}(\tau \rightarrow e\gamma)$ does not strongly depend on ϕ_{M_1} . The effect of ϕ_{M_1} on d_e in case of Fig. (9) is one order of magnitude smaller than the case of Fig. (8) and, like the LF conserving case, is smaller than the effect of ϕ_μ . In contrast to Figs. (7) and (8), in this case $\phi_\mu \simeq \pi/2$ is ruled out by the bound on d_e because the effects of other phases will not be large enough to cancel the effect of $\phi_\mu \simeq \pi/2$. However, for $\phi_\mu < \pi/30$ the effect of ϕ_{M_1} and for $\phi_\mu < \pi/500$ the effects of the phases of LFV mass elements as well as that ϕ_{A_e} can cancel the contribution from ϕ_μ to d_e .

5 Concluding remarks

In this paper, we have discussed the effects of the phase of trilinear A -coupling of the staus, ϕ_{A_τ} , on d_e in the presence of nonzero LFV $e\tau$ elements of the slepton mass matrix. We have shown that for a large portion of the parameter

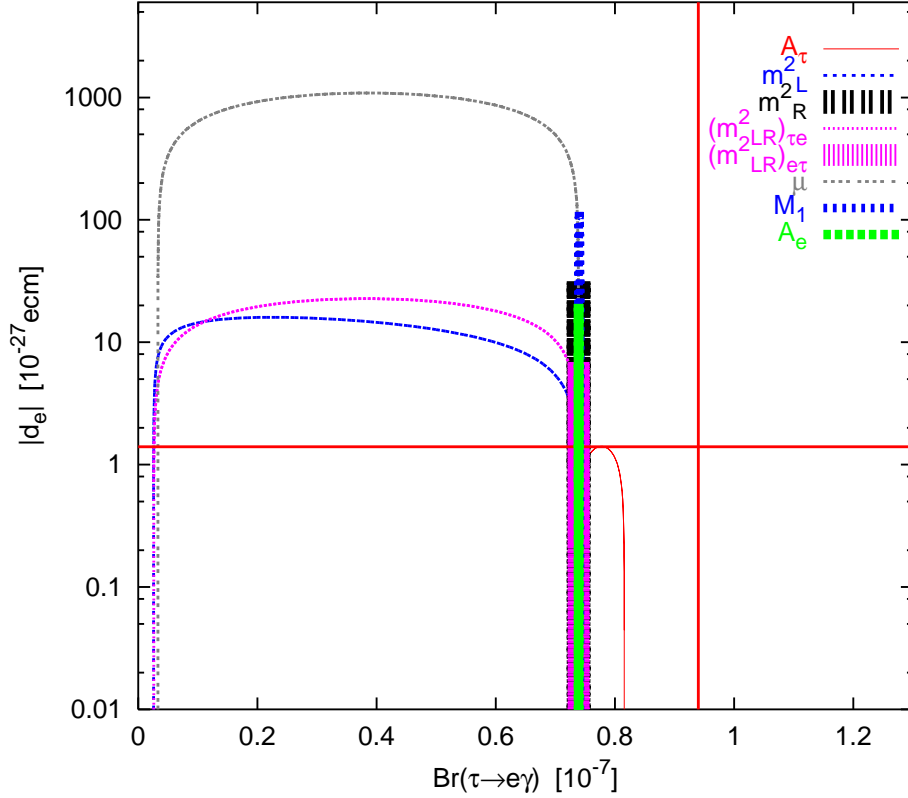


Figure 9: Similarly to Fig. 7 except that here $|(m_L^2)_{e\tau}| = 3000 \text{ GeV}^2$, $|(m_R^2)_{e\tau}| = 50 \text{ GeV}^2$, $|(m_{LR}^2)_{e\tau}| = |A_{e\tau}\langle H_d \rangle = 3 \text{ GeV}^2$ and $|(m_{LR}^2)_{\tau e}| = |A_{\tau e}\langle H_d \rangle = 400 \text{ GeV}^2$. The thin solid red curve, light dotted grey curve, thin dotted blue curve and thin dotted pink curve respectively correspond to varying phases of A_τ , μ , $(m_L^2)_{e\tau}$ and $(m_{LR}^2)_{\tau e}$. The pink, green, black and dark blue thick vertical lines at $\text{Br}(\tau \rightarrow e\gamma) = 7.5 \times 10^{-8}$ (which reach up $d_e = 6.8 \times 10^{-27}, 2 \times 10^{-26}, 3.2 \times 10^{-26}, 1.1 \times 10^{-25} \text{ e cm}$) depict d_e versus $\text{Br}(\tau \rightarrow e\gamma)$ as the phases of respectively $(m_{LR}^2)_{e\tau}$, A_e , $(m_R^2)_{e\tau}$ and M_1 vary between 0 and π . The horizontal line at $d_e = 1.4 \times 10^{-27} \text{ e cm}$ and the vertical line at $\text{Br}(\tau \rightarrow e\gamma) = 9.4 \times 10^{-8}$ show the present experimental limits [13, 15].

space consistent with the present bound on $\text{Br}(\tau \rightarrow e\gamma)$, the contribution of ϕ_{A_τ} to d_e can exceed the present bound by several orders of magnitude. The effect of ϕ_{A_τ} on d_e strongly depends on the ratios of the LFV slepton masses $(m_L^2)_{e\tau}/(m_R^2)_{e\tau}$ and $(m_{LR}^2)_{e\tau}/(m_{LR}^2)_{\tau e}$. In other words, for a given $\text{Br}(\tau \rightarrow e\gamma)$ and $\phi_{A_\tau} = \pm\pi/2$, $|d_e|$ can take any value between zero and a maximum which depends on the value of $\text{Br}(\tau \rightarrow e\gamma)$ [see Figs. (3-a)-(5-a)]. We have shown that for specific case that $(m_{LR}^2)_{e\tau} = (m_{LR}^2)_{\tau e} = 0$ [see Fig. (3-b)] or $(m_L^2)_{e\tau} = (m_R^2)_{e\tau} = 0$ [see Fig. (4-b)], by measuring the asymmetry A_P defined in Eq. (10) we can solve this ambiguity. However, in the general case that all the $e\tau$ elements are nonzero, as shown in Fig. (5), the correlation between A_P and d_e is lost and to solve the ambiguity, extra information is needed.

Assuming that ϕ_{A_τ} is the only source of CP-violation contributing to d_e we have derived bounds on ϕ_{A_τ} for various values of the LFV elements giving rise to $\text{Br}(\tau \rightarrow e\gamma)$ close to the present bound (see Figs. 2 and 6). We have then relaxed this assumption and discussed the possibility of cancelation between contributions of the different phases. We have shown that for large $e\tau$ mass elements saturating the present bounds, the effect of the phase of the Bino, ϕ_{M_1} , on d_e is significantly enhanced which can be explained by the enhancement of the effect of the neutralino exchange diagram by a factor of m_τ/m_e . Taking into account the new bounds on branching ratios of the rare LFV tau decay, we have confirmed the results of [7] that with nonzero LFV effects cancelation scenario makes large values of ϕ_μ consistent with the bound on d_e . We have discussed that the requirement to simultaneously satisfy the bounds on d_e , d_n and d_{Hg} by cancelation imposes a double-folded fine tuning problem.

We have shown that contributions from phases of $(m_L^2)_{e\tau}$, $(m_R^2)_{e\tau}$, $(m_{LR}^2)_{e\tau}$ and $(m_{LR}^2)_{\tau e}$ can cancel the effect of ϕ_{A_τ} on d_e . In summary, although in case of large $e\tau$ elements saturating the bounds from $\text{Br}(\tau \rightarrow e\gamma)$, ϕ_{A_τ} can induce a

large contribution to d_e , still the possibility of cancelation and/or presence of a hierarchy between the LFV $e\tau$ mass matrix elements make even a maximal ϕ_{A_τ} consistent with the d_e bound even if $\text{Br}(\tau \rightarrow e\gamma)$ is found to be close to its present bound. Thus, still there is a hope to observe CP-odd effects at ILC [11].

Acknowledgement

The authors would like to thank M. M. Sheikh-Jabbari for careful reading of the manuscript.

Appendix

In this appendix, we summarize the formulas necessary for calculating A_P , $\text{Br}(\tau \rightarrow e\gamma)$ and d_e . In this paper, we are interested in large LFV $e\tau$ elements. In this parameter range, the mass insertion approximation is not valid and one should work in the mass basis. Here, we first derive the coupling of the sleptons to neutralinos and charginos in the mass basis taking to account the CP-violating phases and mixing. We then present the formulas for A_L and A_R defined in Eq. (7) as well as for the formula for d_e . Throughout this appendix we omit the spinorial indices for simplicity.

In the flavor basis, the mass terms of \tilde{e}_L (the superpartners of the left-handed charged leptons) and \tilde{e}_R (the superpartners of the right-handed charged leptons) can be written as

$$L_{\text{slepton}} = - \begin{pmatrix} \tilde{e}_L^\dagger & \tilde{e}_R^\dagger \end{pmatrix} M_{\tilde{e}}^2 \begin{pmatrix} \tilde{e}_L \\ \tilde{e}_R \end{pmatrix} = - \begin{pmatrix} \tilde{e}_L^\dagger & \tilde{e}_R^\dagger \end{pmatrix} \begin{pmatrix} m_L^2 & m_{LR}^{2\dagger} \\ m_{LR}^2 & m_R^2 \end{pmatrix} \begin{pmatrix} \tilde{e}_L \\ \tilde{e}_R \end{pmatrix} \quad (11)$$

where m_L^2 and m_R^2 are 3×3 Hermitian matrices and m_{LR}^2 is a general complex 3×3 matrix. The elements of these matrices are as follows:

$$(m_L^2)_{ij} = (m_{\tilde{e}_L}^2)_{ij} + (m_{\tilde{e}}^2)_i \delta_{ij} + m_Z^2 \cos 2\beta \left(-\frac{1}{2} + \sin^2 \theta_W\right) \delta_{ij} \quad (12)$$

$$(m_R^2)_{ij} = (m_{\tilde{e}_R}^2)_{ij} + (m_{\tilde{e}}^2)_i \delta_{ij} - m_Z^2 \cos 2\beta \sin^2 \theta_W \delta_{ij} \quad (13)$$

and

$$(m_{LR}^2)_{ij} = m_i (A_i - \mu^* \tan \beta) \delta_{ij} + A_{ij} \langle H_d \rangle \quad (14)$$

where $m_{\tilde{e}_R}^2$ and $m_{\tilde{e}_L}^2$ are respectively the right-handed and left-handed slepton soft supersymmetry breaking mass matrices at the electroweak energy scale and A_{ij} is the trilinear A -coupling [see Eq. (2)]. We can diagonalize the mass matrix of slepton by a 6×6 unitary matrix U^l as

$$[U^l M_{\tilde{e}}^2 (U^l)^{-1}]_{xy} = m_{\tilde{e}_x}^2 \delta_{xy} \quad (15)$$

The slepton mass eigenstate in terms of the chiral weak eigenstate are

$$\tilde{e}_x = \sum_{i=1}^3 [U_{x,i}^l \tilde{e}_{Li} + U_{x,i+3}^l \tilde{e}_{Ri}] \quad (16)$$

Since in the MSSM no $\tilde{\nu}_R$ exists, the neutrino mass matrix will be a 3×3 matrix whose elements can be written as

$$(m_{\tilde{\nu}}^2)_{ij} = (m_{\tilde{e}_L}^2)_{ij} + \left(\frac{1}{2} m_Z^2 \cos 2\beta\right) \delta_{ij} \quad (17)$$

The mass eigenstate, $\tilde{\nu}_x$, is related to the weak eigenstate, $\tilde{\nu}_{Li}$, as

$$\tilde{\nu}_{Li} = \sum_{x=1}^3 U_{x,i}^{\nu*} \tilde{\nu}_x \quad (18)$$

Let us now consider the neutralino masses. The masses of neutralinos in the weak basis can be written as

$$L_{\text{neutralino}} = -\frac{1}{2} (\tilde{X}^0)^T M_{\tilde{N}} \tilde{X}^0 + \text{H.c.}, \quad (19)$$

where $\tilde{X}^0 = (\tilde{B}, \tilde{W}^0, \tilde{H}_d^0, \tilde{H}_u^0)$ and

$$M_{\tilde{N}} = \begin{pmatrix} M_1 & 0 & -m_Z c_\beta s_W & m_Z s_\beta s_W \\ 0 & M_2 & m_Z c_\beta c_W & -m_Z s_\beta c_W \\ -m_Z c_\beta s_W & m_Z c_\beta c_W & 0 & -\mu \\ m_Z s_\beta s_W & -m_Z s_\beta c_W & -\mu & 0 \end{pmatrix}. \quad (20)$$

Here, $s_\beta = \sin \beta$, $c_\beta = \cos \beta$, $s_W = \sin \theta_W$ and $c_W = \cos \theta_W$. The mass matrix $M_{\tilde{N}}$ can be diagonalized as follows:

$$[O_N^* M_{\tilde{N}} O_N^{-1}]_{AB} = M_{\tilde{\chi}_A^0} \delta_{AB} \quad (21)$$

where O_N is a unitary matrix and $M_{\tilde{\chi}_A^0}$ are real positive mass eigenvalues. The mass eigenstates, $\tilde{\chi}_A^0$, in terms of the weak eigenstates, \tilde{X}_B^0 , can be written as

$$\tilde{\chi}_A^0 = (O_N)_{AB} \tilde{X}_B^0. \quad (22)$$

The chargino mass terms can be written as

$$L_{\text{chargino}} = -\frac{1}{2} (\tilde{X}^\pm)^T M_{\tilde{C}} \tilde{X}^\pm + \text{H.c.}, \quad (23)$$

where $(\tilde{X}^\pm)^T = (\tilde{W}^+, \tilde{H}_u^+, \tilde{W}^-, \tilde{H}_d^-)$ and

$$M_{\tilde{C}} = \begin{pmatrix} 0 & C^T \\ C & 0 \end{pmatrix} \quad (24)$$

with

$$C = \begin{pmatrix} M_2 & \sqrt{2} s_\beta m_W \\ \sqrt{2} c_\beta m_W & \mu \end{pmatrix}. \quad (25)$$

The chargino mass matrix C is a general complex matrix which can be diagonalized as

$$U^c C V^{c-1} = \text{diag}(|m_{\tilde{\chi}_1^-}|, |m_{\tilde{\chi}_2^-}|) \quad (26)$$

where U^c and V^c are unitary matrices that satisfy the following relations

$$V^c (C^\dagger C) V^{c-1} = \text{diag}(|m_{\tilde{\chi}_1^-}|^2, |m_{\tilde{\chi}_2^-}|^2) = U^c (C C^\dagger) U^{c-1}. \quad (27)$$

Notice that we have defined U^c and V^c in a way that the elements of the diagonal matrix $U^c C V^{c-1}$ are real positive. Eqs. (26,27) are invariant under

$$U^c \rightarrow \begin{pmatrix} e^{i\alpha_1} & 0 \\ 0 & e^{i\alpha_2} \end{pmatrix} U^c, \quad V^c \rightarrow \begin{pmatrix} e^{i\alpha_1} & 0 \\ 0 & e^{i\alpha_2} \end{pmatrix} V^c. \quad (28)$$

Thus, there is an ambiguity in the definition of U^c and V^c but the final results do not depend on the unphysical phases α_1 and α_2 , as expected.

The mass eigenstates are related to the gauge eigenstates through

$$\begin{pmatrix} \tilde{\chi}_1^+ \\ \tilde{\chi}_2^+ \end{pmatrix} = V^c \begin{pmatrix} \tilde{W}^+ \\ \tilde{H}_u^+ \end{pmatrix} \quad \begin{pmatrix} \tilde{\chi}_1^- \\ \tilde{\chi}_2^- \end{pmatrix} = U^{c*} \begin{pmatrix} \tilde{W}^- \\ \tilde{H}_d^- \end{pmatrix}. \quad (29)$$

Within the framework of the MSSM, the lepton-slepton-neutralino coupling in the mass basis and in the Weyl representation can be written as

$$L_{int}^{(n)} = \sum_{x=1}^6 e_{Li}^\dagger (N_{iAx}^R) \tilde{\chi}_A^{0\dagger} \tilde{e}_x + e_{Ri}^\dagger (N_{iAx}^L) \tilde{\chi}_A^0 \tilde{e}_x + \text{H.c.}, \quad (30)$$

where the couplings are

$$\begin{aligned} N_{iAx}^R &= -\frac{g_2}{\sqrt{2}} ([-(O_N)_{A2} - (O_N)_{A1} \tan \theta_W] U_{x,i}^{l*} + \frac{m_{e_i}}{m_W \cos \beta} (O_N)_{A3} U_{x,i+3}^{l*}) \\ N_{iAx}^L &= -\frac{g_2}{\sqrt{2}} [2(O_N)_{A1}^* \tan \theta_W U_{x,i+3}^{l*} + \frac{m_{e_i}}{m_W \cos \beta} (O_N)_{A3}^* U_{x,i}^{l*}]. \end{aligned} \quad (31)$$

The lepton-slepton-chargino coupling can be written as

$$L_{int}^{(c)} = \sum_{x=1}^3 e_{Li}^\dagger (C_{iAx}^R) \tilde{\chi}_A^{+\dagger} \tilde{\nu}_x + e_{Ri}^\dagger (C_{iAx}^L) \tilde{\chi}_A^- \tilde{\nu}_x + \text{H.c.} \quad (32)$$

where the couplings are

$$\begin{aligned} C_{iAx}^R &= -g_2 U_{x,i}^{\nu*} V_{A,1}^c \\ C_{iAx}^L &= \frac{m_{e_i}}{\sqrt{2} m_W \cos \beta} g_2 U_{x,i}^{\nu*} U_{A,2}^c. \end{aligned} \quad (33)$$

Let us now discuss the formulas for $(A_L)_{ij}$ and $(A_R)_{ij}$ defined as

$$e \epsilon_\alpha^\dagger m_\tau \bar{e}_i \sigma^{\alpha\beta} q_\beta [(A_L)_{ij} P_L + (A_R)_{ij} P_R] e_j + \text{H.c.} \quad (34)$$

where $\sigma^{\alpha\beta} = \frac{i}{2}[\gamma^\alpha, \gamma^\beta]$ and q_β is the four-momentum of the photon. P_L and P_R are respectively the left and right projection matrices. Notice that $(A_L)_{e\tau}$ and $(A_R)_{e\tau}$ defined in (7) are the $e\tau$ component of the 3×3 matrices $(A_L)_{ij}$ and $(A_R)_{ij}$. For the CP-conserving case the formulas for A_L and A_R have been developed in [16]. We have rederived the formulae for the CP-violating case. It is convenient to decompose A_L and A_R as follows

$$A_{L,R} = A_{L,R}^{(n)} + A_{L,R}^{(c)} \quad (35)$$

where $A_{L,R}^{(n)}$ and $A_{L,R}^{(c)}$ respectively come from neutralino-slepton and chargino-sneutrino loops. In terms of the coupling in the mass basis we can write

$$\begin{aligned} (A_L^{(n)})_{ij} = & \sum_{A=1}^4 \sum_{x=1}^6 \frac{1}{32\pi^2} \frac{1}{m_{\tilde{e}_x}^2} [N_{iAx}^L N_{jAx}^{L*} \frac{1}{6(1-y_{Ax})^4} \\ & \times (1 - 6y_{Ax} + 3y_{Ax}^2 + 2y_{Ax}^3 - 6y_{Ax}^2 \ln y_{Ax}) \\ & + N_{iAx}^L N_{jAx}^{R*} \frac{M_{\tilde{\chi}_A^0}}{m_{e_j}} \frac{1}{(1-y_{Ax})^3} (1 - y_{Ax}^2 + 2y_{Ax} \ln y_{Ax})], \end{aligned} \quad (36)$$

where $y_{Ax} = M_{\tilde{\chi}_A^0}^2 / m_{\tilde{e}_x}^2$ and

$$\begin{aligned} (A_L^{(c)})_{ij} = & \sum_{A=1}^2 \sum_{x=1}^3 - \frac{1}{32\pi^2} \frac{1}{m_{\tilde{\nu}_x}^2} [C_{iAx}^L C_{jAx}^{L*} \frac{1}{6(1-z_{Ax})^4} \\ & \times (2 + 3z_{Ax} - 6z_{Ax}^2 + z_{Ax}^3 + 6z_{Ax} \ln z_{Ax}) \\ & + C_{iAx}^L C_{jAx}^{R*} \frac{M_{\tilde{\chi}_A^-}}{m_{e_j}} \frac{1}{(1-z_{Ax})^3} (-3 + 4z_{Ax} - z_{Ax}^2 - 2 \ln z_{Ax})] \end{aligned} \quad (37)$$

$z_{Ax} = M_{\tilde{\chi}_A^-}^2 / m_{\tilde{\nu}_x}^2$. Finally

$$A_R^{(n)} = A_L^{(n)}|_{L \leftrightarrow R} \quad A_R^{(c)} = A_L^{(c)}|_{L \leftrightarrow R}. \quad (38)$$

Notice that the forms of the above formulas are similar to those in [16]; however, the couplings $N^{R,L}$ and $C^{R,L}$ are slightly different because of the nonzero CP-violating phases.

Now, let us summarize the formula for d_e . It is also convenient to decompose d_e into the neutralino-exchange and chargino-exchange contributions as follows:

$$d_e = d_e^{(n)} + d_e^{(c)}.$$

These contributions have been extensively studied in the literature including in [26] which give

$$d_e^{(c)} = -\frac{e}{(4\pi)^2} \sum_{A=1}^2 \sum_{x=1}^3 \text{Im}(C_{eAx}^L C_{eAx}^{R*}) \frac{m_{\tilde{\chi}_A^-}}{m_{\tilde{\nu}_x}^2} A \left(\frac{m_{\tilde{\chi}_A^-}^2}{m_{\tilde{\nu}_x}^2} \right)$$

$$d_e^{(n)} = -\frac{e}{(4\pi)^2} \sum_{A=1}^4 \sum_{x=1}^6 \text{Im}(N_{eAx}^L N_{eAx}^{R*}) \frac{m_{\tilde{\chi}_A^0}}{m_{\tilde{e}_x}^2} B \left(\frac{m_{\tilde{\chi}_A^0}^2}{m_{\tilde{e}_x}^2} \right)$$

where

$$A(x) = \frac{1}{2(1-x)^2} \left(3 - x + \frac{2 \ln x}{1-x} \right)$$

and

$$B(x) = \frac{1}{2(1-x)^2} \left(1 + x + \frac{2x \ln x}{1-x} \right).$$

References

- [1] F. Hoogeveen, Nucl. Phys. B **341** (1990) 322. M. E. Pospelov and I. B. Khriplovich, Sov. J. Nucl. Phys. **53** (1991) 638 [Yad. Fiz. **53** (1991) 1030]; M. J. Booth, arXiv:hep-ph/9301293.
- [2] D. Kawall, F. Bay, S. Bickman, Y. Jiang and D. DeMille, AIP Conf. Proc. **698** (2004) 192; D. Kawall, F. Bay, S. Bickman, Y. Jiang and D. DeMille, Phys. Rev. Lett. **92** (2004) 133007 [arXiv:hep-ex/0309079].
- [3] S. K. Lamoreaux, Phys. Rev. D **66** (2002) 010001 arXiv:nucl-ex/0109014.

- [4] G. Altarelli, L. Baulieu, N. Cabibbo, L. Maiani and R. Petronzio, Nucl. Phys. B **125** (1977) 285 [Erratum-ibid. B **130** (1977) 516]; S. M. Bilenky, S. T. Petcov and B. Pontecorvo, Phys. Lett. B **67** (1977) 309; S. T. Petcov, Sov. J. Nucl. Phys. **25** (1977) 340 [Yad. Fiz. **25** (1977) ERRAT,25,698.1977 ERRAT,25,1336.1977) 641]; W. J. Marciano and A. I. Sanda, Phys. Lett. B **67** (1977) 303.
- [5] <http://www.slac.stanford.edu/BFROOT/>;
<http://belle.kek.jp/>;<http://meg.web.psi.ch/>
- [6] K. A. Olive, M. Pospelov, A. Ritz and Y. Santoso, Phys. Rev. D **72** (2005) 075001 [arXiv:hep-ph/0506106]; S. Abel, S. Khalil and O. Lebedev, Nucl. Phys. B **606** (2001) 151 [arXiv:hep-ph/0103320]; T. Falk *et al.*, Nucl. Phys. B **560** (1999) 3 [arXiv:hep-ph/9904393]; A. Afanasev, C. E. Carlson and C. Wahlquist, Phys. Rev. D **61** (2000) 034014 [arXiv:hep-ph/9903493]; T. Ibrahim and P. Nath, Phys. Lett. B **418** (1998) 98 [arXiv:hep-ph/9707409]; M. Brhlik, G. J. Good and G. L. Kane, Phys. Rev. D **59** (1999) 115004 [arXiv:hep-ph/9810457]; A. Bartl *et al.*, Phys. Rev. D **60** (1999) 073003 [arXiv:hep-ph/9903402]; T. Falk, K. A. Olive, M. Pospelov and R. Roiban, Nucl. Phys. B **560** (1999) 3 [arXiv:hep-ph/9904393].
- [7] S. Y. Ayazi and Y. Farzan, Phys. Rev. D **74** (2006) 055008 [arXiv:hep-ph/0605272]; S. Y. Ayazi, arXiv:hep-ph/0611056.
- [8] P. Nath, Phys. Rev. Lett. **66** (1991) 2565 ; Y. Kizukuri and N. Oshimo, Phys. Rev. D **46** (1992) 3025; V. A. Kuzmin, V. A. Rubakov and M. E. Shaposhnikov, Phys. Lett. B **155**, 36 (1985); V. Cirigliano, S. Profumo and M. J. Ramsey-Musolf, JHEP **0607**, 002 (2006) [arXiv:hep-ph/0603246] K. A. Olive, M. Pospelov, A. Ritz and Y. Santoso, Phys. Rev. D **72** (2005) 075001 [arXiv:hep-ph/0506106]; T. Falk and

- K. A. Olive, Phys. Lett. B **375** (1996) 196 [arXiv:hep-ph/9602299];
T. Ibrahim and P. Nath, arXiv:hep-ph/0210251.
- [9] A. Bartl, W. Majerotto, W. Porod and D. Wyler, Phys. Rev. D **68**
(2003) 053005 [arXiv:hep-ph/0306050]; W. Porod, *Prepared for Inter-
national Workshop on Astroparticle and High-Energy Physics (AHEP-
2003), Valencia, Spain, 14-18 Oct 2003*.
- [10] A. Bartl, K. Hidaka, T. Kernreiter and W. Porod, Phys. Rev. D **66**
(2002) 115009 [arXiv:hep-ph/0207186]; T. Gajdosik, R. M. Godbole and
S. Kraml, JHEP **0409** (2004) 051 [arXiv:hep-ph/0405167]; O. Kittel,
arXiv:hep-ph/0504183; A. Bartl, T. Kernreiter and O. Kittel, Phys.
Lett. B **578** (2004) 341 [arXiv:hep-ph/0309340].
- [11] A. Bartl and S. Hesselbach, Pramana **63** (2004) 1101 [arXiv:hep-
ph/0407178]; S. Hesselbach, O. Kittel, G. A. Moortgat-Pick and
W. Oller, Eur. Phys. J. C **33** (2004) S746 [arXiv:hep-ph/0310367];
E. Boos, H. U. Martyn, G. A. Moortgat-Pick, M. Sachwitz, A. Sher-
stnev and P. M. Zerwas, Eur. Phys. J. C **30** (2003) 395 [arXiv:hep-
ph/0303110]; A. Freitas *et al.*, arXiv:hep-ph/0211108.
- [12] Y. Farzan, arXiv:hep-ph/0701106.
- [13] W.-M. Yao *et al.*, J. Phys. G **33** (2006) 1.
- [14] D. Chang, W. Y. Keung and A. Pilaftsis, Phys. Rev. Lett. **82** (1999)
900 [Erratum-ibid. **83** (1999) 3972] [arXiv:hep-ph/9811202].
- [15] S. Banerjee, arXiv:hep-ex/0702017; *see also*, B. Aubert *et al.*
[BABAR Collaboration], Phys. Rev. Lett. **96** (2006) 041801 [arXiv:hep-
ex/0508012]; K. Abe *et al.* [Belle Collaboration], arXiv:hep-ex/0609049.

- [16] J. Hisano, T. Moroi, K. Tobe and M. Yamaguchi, Phys. Rev. D **53** (1996) 2442 [arXiv:hep-ph/9510309].
- [17] R. Kitano and Y. Okada, Phys. Rev. D **63** (2001) 113003 [arXiv:hep-ph/0012040].
- [18] A. De Roeck *et al.*, arXiv:hep-ph/0508198.
- [19] F. Borzumati and A. Masiero, Phys. Rev. Lett. **57** (1986) 961; Y. Farzan, Phys. Rev. D **69** (2004) 073009 [arXiv:hep-ph/0310055].
- [20] R. Barbieri and L. J. Hall, Phys. Lett. B **338** (1994) 212 [arXiv:hep-ph/9408406]; R. Barbieri, L. J. Hall and A. Strumia, Nucl. Phys. B **445** (1995) 219 [arXiv:hep-ph/9501334].
- [21] M. Guchait, J. Kalinowski and P. Roy, Eur. Phys. J. C **21** (2001) 163 [arXiv:hep-ph/0103161]; A. Bartl *et al.* [ECFA/DESY SUSY Collaboration], arXiv:hep-ph/0301027.
- [22] M. Pospelov and A. Ritz, Phys. Rev. D **63** (2001) 073015 [arXiv:hep-ph/0010037]; J. Hisano and Y. Shimizu, Phys. Rev. D **70** (2004) 093001 [arXiv:hep-ph/0406091].
- [23] T. Falk, K. A. Olive, M. Pospelov and R. Roiban, Nucl. Phys. B **560** (1999) 3 [arXiv:hep-ph/9904393]; J. Hisano, M. Kakizaki, M. Nagai and Y. Shimizu, Phys. Lett. B **604** (2004) 216 [arXiv:hep-ph/0407169].
- [24] O. Lebedev, K. A. Olive, M. Pospelov and A. Ritz, Phys. Rev. D **70**, 016003 (2004) [arXiv:hep-ph/0402023];
- [25] D. A. Demir and Y. Farzan, JHEP **0510** (2005) 068 [arXiv:hep-ph/0508236]; D. A. Demir and Y. Farzan, arXiv:hep-ph/0610181.

- [26] T. Ibrahim and P. Nath, Phys. Rev. D **57** (1998) 478 [Erratum-ibid. D **58** (1998 ERRAT,D60,079903.1999 ERRAT,D60,119901.1999) 019901] [arXiv:hep-ph/9708456]; S. Abel, S. Khalil and O. Lebedev, Nucl. Phys. B **606** (2001) 151 [arXiv:hep-ph/0103320]; J. R. Ellis, J. Hisano, M. Raidal and Y. Shimizu, Phys. Lett. B **528** (2002) 86 [arXiv:hep-ph/0111324].